

Carbon nanostructure-based saturable absorber mirror for a diode-pumped 500-MHz femtosecond Yb:KLu(WO₄)₂ laser

Sun Young Choi,¹ Jun Wan Kim,¹ Mi Hye Kim,¹ Dong-Il Yeom,¹ Byung Hee Hong,² Xavier Mateos,³ Magdalena Aguiló,³ Francesc Díaz,³ Valentin Petrov,⁴ Uwe Griebner,⁴ and Fabian Rotermund^{1,*}

¹Department of Energy Systems Research & Department of Physics, Ajou University, Suwon 443-749, South Korea

²Department of Chemistry, Seoul National University, Seoul 151-742, South Korea

³Física i Cristallografia de Materials (FiCMA), Universitat Rovira i Virgili (URV), Marcelli Domingo, s/n, E-43007 Tarragona, Spain

⁴Max Born Institute for Nonlinear Optics & Short Pulse Spectroscopy, 12489 Berlin, Germany
rotermun@ajou.ac.kr

Abstract: We report a diode-pumped Yb:KLu(WO₄)₂ (Yb:KLuW) laser passively mode-locked by employing a carbon nanostructure-based multifunctional saturable absorber mirror. Two types of carbon nanostructures, single-walled carbon nanotubes (SWCNTs) and graphene, were deposited on a single dielectric mirror and applied both for stable mode-locking of the Yb:KLuW laser near 1050 nm in a compact cavity configuration. The carbon nanostructure mode-locked laser delivers 157-fs pulses with output powers of up to 85 mW at a repetition rate of 500 MHz.

©2014 Optical Society of America

OCIS codes: (140.4050) Mode-locked lasers; (140.3480) Lasers, diode-pumped; (320.7090) Ultrafast lasers; (160.4330) Nonlinear optical materials.

References and links

1. H. Liu, J. Nees, and G. Mourou, "Diode-pumped Kerr-lens mode-locked Yb:KY(WO₄)₂ laser," *Opt. Lett.* **26**(21), 1723–1725 (2001).
2. A. A. Lagatsky, C. T. A. Brown, and W. Sibbett, "Highly efficient and low threshold diode-pumped Kerr-lens mode-locked Yb:KYW laser," *Opt. Express* **12**(17), 3928–3933 (2004).
3. A. Agnesi, A. Greborio, F. Pirzio, and G. Reali, "80-fs Nd:silicate glass laser pumped by a single-mode 200-mW diode," *Opt. Express* **18**(10), 10098–10103 (2010).
4. A. Agnesi, A. Greborio, F. Pirzio, G. Reali, S. Y. Choi, F. Rotermund, U. Griebner, and V. Petrov, "99 fs Nd:glass laser mode-locked with carbon nanotube saturable absorber mirror," *Appl. Phys. Express* **3**(11), 112702 (2010).
5. A. Schmidt, S. Rivier, G. Steinmeyer, J. H. Yim, W. B. Cho, S. Lee, F. Rotermund, M. C. Pujol, X. Mateos, M. Aguiló, F. Díaz, V. Petrov, and U. Griebner, "Passive mode locking of Yb:KLuW using a single-walled carbon nanotube saturable absorber," *Opt. Lett.* **33**(7), 729–731 (2008).
6. H.-W. Yang, C. Kim, S. Y. Choi, G.-H. Kim, Y. Kobayashi, F. Rotermund, and J. Kim, "1.2-GHz repetition rate, diode-pumped femtosecond Yb:KYW laser mode-locked by a carbon nanotube saturable absorber mirror," *Opt. Express* **20**(28), 29518–29523 (2012).
7. E. Ugolotti, A. Schmidt, V. Petrov, J. W. Kim, D.-I. Yeom, F. Rotermund, S. Bae, B. H. Hong, A. Agnesi, C. Fiebig, G. Erbert, X. Mateos, M. Aguiló, F. Díaz, and U. Griebner, "Graphene mode-locked femtosecond Yb:KLuW laser," *Appl. Phys. Lett.* **101**(16), 161112 (2012).
8. U. Keller, K. J. Weingarten, F. X. Kärtner, D. Kopf, B. Braun, I. D. Jung, R. Fluck, C. Hönninger, N. Matuschek, and J. Aus der Au, "Semiconductor saturable absorber mirrors (SESAM's) for femtosecond to nanosecond pulse generation in solid-state lasers," *IEEE J. Sel. Top. Quantum Electron.* **2**(3), 435–453 (1996).
9. D. Kopf, G. Zhang, R. Fluck, M. Moser, and U. Keller, "All-in-one dispersion-compensating saturable absorber mirror for compact femtosecond laser sources," *Opt. Lett.* **21**(7), 486–488 (1996).
10. J. W. Nicholson, R. S. Windeler, and D. J. Digiovanni, "Optically driven deposition of single-walled carbon-nanotube saturable absorbers on optical fiber end-faces," *Opt. Express* **15**(15), 9176–9183 (2007).
11. S. Y. Choi, H. Jeong, B. H. Hong, F. Rotermund, and D.-I. Yeom, "All-fiber dissipative soliton laser with 10.2 nJ pulse energy using an evanescent field interaction with graphene saturable absorber," *Laser Phys. Lett.* **11**(1), 015101 (2014).
12. R. Mary, G. Brown, S. J. Beecher, R. R. Thomson, D. Popa, Z. Sun, F. Torrisi, T. Hasan, S. Milana, F. Bonaccorso, A. C. Ferrari, and A. K. Kar, "Evanescent-wave coupled right angled buried waveguide: Applications in carbon nanotube mode-locking," *Appl. Phys. Lett.* **103**(22), 221117 (2013).

13. T. R. Schibli, K. Minoshima, H. Katura, E. Itoga, N. Minami, S. Kazaoui, K. Miyashita, M. Tokumoto, and Y. Sakakibara, "Ultrashort pulse-generation by saturable absorber mirrors based on polymer-embedded carbon nanotubes," *Opt. Express* **13**(20), 8025–8031 (2005).
14. W. B. Cho, J. H. Yim, S. Y. Choi, S. Lee, A. Schmidt, G. Steinmeyer, U. Griebner, V. Petrov, D.-I. Yeom, K. Kim, and F. Rotermund, "Boosting the nonlinear optical response of carbon nanotube saturable absorber for broadband mode-locking of bulk lasers," *Adv. Funct. Mater.* **20**(12), 1937–1943 (2010).
15. A. Schmidt, S. Y. Choi, D.-I. Yeom, F. Rotermund, X. Mateos, M. Segura, F. Diaz, V. Petrov, and U. Griebner, "Femtosecond pulses near 2 μm from a Tm:KLuW laser mode-locked by a single-walled carbon nanotube saturable absorber," *Appl. Phys. Express* **5**(9), 092704 (2012).
16. I. H. Baek, H. W. Lee, S. Bae, B. H. Hong, Y. H. Ahn, D.-I. Yeom, and F. Rotermund, "Efficient mode-locking of sub-70-fs Ti:sapphire laser by graphene saturable absorber," *Appl. Phys. Express* **5**(3), 032701 (2012).
17. W. B. Cho, J. W. Kim, H. W. Lee, S. Bae, B. H. Hong, S. Y. Choi, I. H. Baek, K. Kim, D.-I. Yeom, and F. Rotermund, "High-quality, large-area monolayer graphene for efficient bulk laser mode-locking near 1.25 μm ," *Opt. Lett.* **36**(20), 4089–4091 (2011).
18. M. N. Cizmeciyan, J. W. Kim, S. Bae, B. H. Hong, F. Rotermund, and A. Sennaroglu, "Graphene mode-locked femtosecond Cr:ZnSe laser at 2500 nm," *Opt. Lett.* **38**(3), 341–343 (2013).
19. S. Bae, H. Kim, Y. Lee, X. Xu, J.-S. Park, Y. Zheng, J. Balakrishnan, T. Lei, H. R. Kim, Y. I. Song, Y.-J. Kim, K. S. Kim, B. Özyilmaz, J.-H. Ahn, B. H. Hong, and S. Iijima, "Roll-to-roll production of 30-inch graphene films for transparent electrodes," *Nat. Nanotechnol.* **5**(8), 574–578 (2010).
20. J. H. Yim, W. B. Cho, S. Lee, Y. H. Ahn, K. Kim, H. Lim, G. Steinmeyer, V. Petrov, U. Griebner, and F. Rotermund, "Fabrication and characterization of ultrafast carbon nanotube saturable absorber for solid-state laser mode-locking near 1 μm ," *Appl. Phys. Lett.* **93**(16), 161106 (2008).

1. Introduction

Diode-pumped ultrafast solid-state lasers operating at wavelengths near 1 μm provide a cost-effective solution for various applications compatible with moderate average powers, such as optical coherence tomography, nonlinear microscopy, THz generation and detection, and seeding of ultrafast amplifiers. In recent years, Yb- and Nd-doped gain media have been widely used for 1- μm diode-pumped mode-locked lasers [1–4]. The Yb³⁺ ion provides a small quantum defect as a result of close pump and laser wavelengths, leading to low thermal load and high efficiency. In particular, Yb-doped double tungstate gain media such as Yb:KY(WO₄)₂ (Yb:KYW) and Yb:KLu(WO₄)₂ (Yb:KLuW) have enabled the generation of stable broadband and tunable pulses. Recently, carbon nanostructure-based saturable absorbers (SAs) based on single-walled carbon nanotubes (SWCNTs) and graphene have attracted much attention for mode-locking of Yb-doped bulk lasers [5–7]. The carbon nanostructures turned out to be promising materials applicable as saturable absorbers for mode-locking of various lasers due to broadband coverage, high nonlinearity, and ultrafast response time. Based on these properties excellent mode-locking performance was demonstrated comparable to the results achieved with semiconductor saturable absorber mirrors (SESAMs) [8,9]. The applicability of carbon nanostructures as mode-locker is more flexible than SESAMs. Those kinds of SAs can be fabricated in various types, not even for reflection but also for transmission and evanescent wave interaction [10–12]. Furthermore, ultrabroad absorption behavior of carbon nanostructures renders them suitable for mode-locking in diverse cavity geometries in a wide spectral range from the near- to mid-infrared [10–18].

In the present work, we demonstrate a diode-pumped compact femtosecond Yb:KLuW laser, passively mode-locked by employing carbon nanostructure-based SAMs. Two types of carbon nanostructures, SWCNTs and graphene, are deposited on a single dielectric mirror and employed both for mode-locking. Well-dispersed SWCNT/polymer composite and large-area monolayer graphene sheet are first synthesized to fabricate SAs in suitable structures for a compact laser cavity. The 30-cm-long laser generates stable femtosecond pulses near 1 μm at a repetition rate of 500 MHz.

2. Fabrication of carbon nanostructure-based saturable absorber mirror

Both the prepared SWCNT/polymer composite and the monolayer graphene sheet are deposited on a single high-reflection-coated dielectric mirror. For fabrication of SWCNT-SAM, commercially available arc-discharged SWCNT powder (Meijo Nano Carbon Co., Ltd) which shows two broad absorption bands, corresponding to interband transitions of

semiconducting SWCNTs, near 1 and 1.9 μm is used as the starting material. The SWCNT powder is dispersed via ultrasonic agitation in 1,2-dichlorobenzene (DCB) at concentration of 0.1 mg/ml for few hours. The SWCNT dispersion solution is then centrifuged for 30 minutes to remove bundled large particles, since strong bundling and curling of nanotubes leads to undesired scattering. Subsequently, the well-dispersed SWCNT solution is mixed with poly(methyl methacrylate) (PMMA). The SWCNT/PMMA composite solution is finally spin-coated on a quarter of 1/2-inch mirror with a thickness of about 500 nm. A similar SWCNT-based SAM has been successfully employed for mode-locking of a Yb:KYW laser in our previous investigation [6]. However, the SWCNT-SAM used in the present work is fabricated in a slightly different way. Few parameters, such as the dispersion degree of SWCNT solution and the thickness of SWCNT/PMMA composite layer, are optimized to enhance the performance of the SWCNT-SAM in the present laser cavity. For fabrication of graphene-SA simultaneously on the same mirror, high-quality monolayer graphene is first synthesized by the thermal chemical vapor deposition (TCVD) method [19]. On the top of as-grown monolayer graphene on copper foil, a thin PMMA layer is spin-coated to support graphene during the wet transfer onto the mirror. A copper foil is then etched away in an ammonium persulfate solution and rinsed off with deionized water. The water-floated graphene/PMMA thin-film is finally transferred to another quarter of the mirror. The fabricated SAM with SWCNTs and graphene is used as the end mirror in the laser experiment. Since the 0.34-nm-thin monolayer graphene will not experience sufficiently high mode field at the end of the standing-wave laser cavity, a PMMA buffer layer with an adequate thickness is deposited on the mirror prior to graphene transfer. The graphene-SAM shows a sandwich structure, in which the monolayer graphene is located between the PMMA layers. The total thickness of graphene-SAM is about 700 nm. Same SWCNTs and graphene used as saturable absorber in the present experiment were deposited on the transparent substrates to investigate their nonlinear optical characteristics in transmission. Similar to previous studies [6,20] the SWCNTs possess saturation fluence of about $10 \mu\text{J}/\text{cm}^2$, modulation depth of about 0.3%, and non-saturable loss of 1%. The nonlinear response is measured to be $\tau_1 \approx 150 \text{ fs}$ and $\tau_2 \approx 1.2 \text{ ps}$, respectively. For the case of monolayer graphene, saturation fluence of about $55 \mu\text{J}/\text{cm}^2$, modulation depth of about 0.6%, and non-saturable loss of 1.4% are measured, while the nonlinear response of the graphene-SA is comparable to the case of SWCNT-SA.

The structure of the fabricated SAM is schematically depicted in Fig. 1(a). The single, high reflecting dielectric mirror contains three areas: one coated with SWCNTs and one with a graphene absorber layer whereas the third part is without carbon nanostructure coating. This kind of structuring enables one easily to compare the laser performance with the absorber devices and in the continuous-wave (cw) regime by simple translation of the mirror. Figure 1(b) shows a photograph of the multi-functional dielectric mirror.

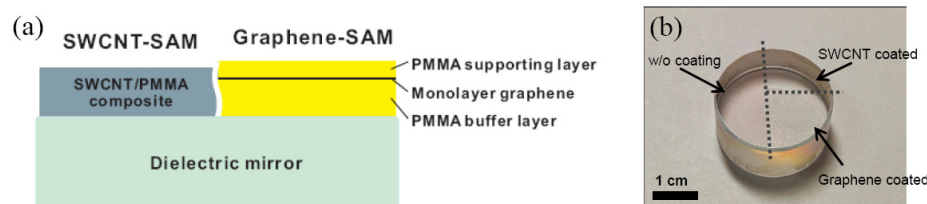


Fig. 1. (a) Schematic of the carbon nanostructure-based multifunctional SAM and (b) photograph of the fabricated SAM (a three-area containing single dielectric mirror partially coated with SWCNTs and a graphene layer).

3. Results with the carbon nanostructure mode-locked Yb:KLuW laser

Figure 2 shows the scheme of the passively mode-locked Yb:KLuW laser by using SWCNT- and graphene-SAM. The resonator configuration is an extended dispersion-compensated asymmetric z-cavity. A single-mode pump beam from a fiber-pigtailed 980-nm laser diode (LD) is collimated and focused onto the laser crystal by a convex lens of $f = 7.5$ cm. The active medium is 3-mm-thick 5% Yb-doped KLuW crystal oriented for Brewster angle polarization parallel to the N_m -optical axis. The pump beam from the LD is linearly polarized via polarization-maintaining fiber (PMF) and matches the polarization state with a half-wave plate to the laser crystal. The maximum pump power delivered to the laser gain medium is 860 mW. The Yb:KLuW crystal is mounted on a base plate without active cooling and placed near the focus of the folded cavity between two concave mirrors M1 and M2 with radius of curvature (ROC) of 50 mm. The measured pump beam waist in the crystal is $26 \mu\text{m}$, whereas the beam waist of the laser mode is calculated to be about $28 \mu\text{m}$. The three-area dielectric mirror containing the SWCNT- and graphene-coated SAM is mounted on a 2-axis translation stage and inserted at the end of laser cavity. An output coupler (OC) of $T = 1\%$ is installed at the other end of resonator. The mode size on the SAM can be varied by changing the distance ratio of M1-OC and M2-SAM to achieve sufficient fluence for saturable absorption. Note that the beam size at the cavity end is much smaller on the shorter-arm side of our asymmetric cavity configuration. To avoid possible damage of SWCNT and graphene absorber layer, the SAM is implemented in the longer cavity arm. Depending on the absorber position, the beam waist on the SAM could be varied between 40 and $90 \mu\text{m}$. No damage of the SAM is observed in this configuration. To compensate the cavity dispersion, the M2-SAM arm is folded by a Gires-Tournois interferometer (GTI) mirror M3 with negative dispersion of -1300 fs^2 per bounce. The contribution of both SWCNT and graphene layers to the intra-cavity dispersion is negligible because the thickness is only 500 to 700 nm . Taking into account the dispersion of the Yb:KLuW crystal ($+110 \text{ fs}^2/\text{mm}$) and air ($+0.016 \text{ fs}^2/\text{mm}$), the resulting net cavity dispersion for one round trip is about -1930 fs^2 near 1050 nm . The total cavity length of the laser is about 30 cm and the mode-locked laser operates stable with both SWCNT- and graphene-SAM when the M1-M2 separation is set to operate in the second stability region.

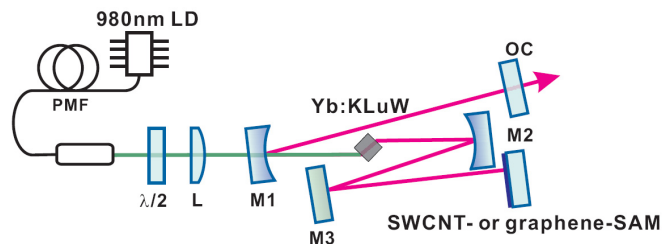


Fig. 2. Setup of the Yb:KLuW laser mode-locked by SWCNT- & graphene-SAM. $\lambda/2$: half-wave plate, L: convex lens with $f = 7.5$ cm, M1 & M2: dielectric curved mirror with ROC = 50 mm, M3: GTI flat mirror with $-1300 \text{ fs}^2/\text{mm}$ dispersion at 1050 nm , and OC: 1% output coupler.

Using the area of the multi-functional mirror without SA coating (Fig. 1(b)) cw lasing starts at an incident pump power of 235 mW , whereas the laser threshold with SWCNT-SAM and graphene-SAM is increases to 300 and 325 mW , respectively. A maximum cw output power of 215 mW is achieved without SAM. The average output power of the mode-locked Yb:KLuW laser with the SWCNT-SAM as well as with the graphene-SAM are measured versus the incident pump power (Fig. 3). Self-starting mode-locked operation is observed with both SAMs by increasing the pump power. In the case with SWCNT-SAM, mode-locking is easily achieved due to relatively low saturation fluence and stably maintains the pulse generation. The laser could be easily mode-locked without multiple pulsing in the broad power range starting from slightly above the lasing threshold up to the maximum output

power shown in Fig. 3. The mode-locking threshold is measured to be 330 mW of the input pump power. In the identical cavity configuration, graphene-SAM does not experience sufficient fluence to initiate pulsation. Increasing the M2-SAM separation, that moves the laser operation range to the edge of the second stability zone of resonator, reduces the mode size on the SAM and increases the fluence making mode-locked operation self-starting. The mode-locking starts at the pump power of 445 mW. The threshold is a bit higher than in the case with SWCNT-SAM. The maximum average output power of the SWCNT- and graphene-SAM mode-locked Yb:KLuW laser with 1% OC is 85 and 73 mW and the corresponding slope efficiency 15.2% and 13.7%, respectively. At the relatively low modulation depths the slope does not change when entering the mode-locked regime. The insets of Fig. 3 show the beam profiles of the SWCNT-SAM and graphene-SAM mode-locked laser output recorded at a distance of 110 mm from OC, indicating nice TEM₀₀-mode profiles in both cases. The SWCNT- and graphene-SAM mode-locked laser operate stable for hours with a negligible power variation.

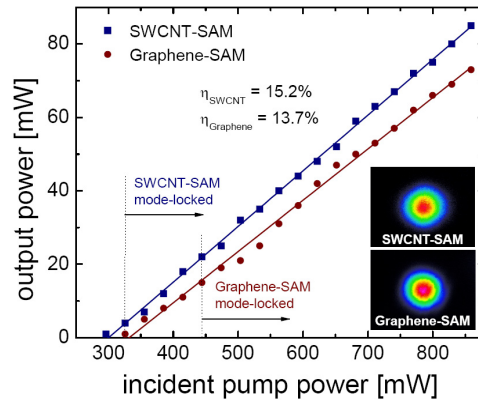


Fig. 3. Average output power of the Yb:KLuW laser mode-locked by SWCNT-SAM (squares) and graphene-SAM (circles) with 1% output coupling and the beam profiles recorded for both SAMs in mode-locked operation (inset). η denotes slope efficiency.

Figure 4 shows the autocorrelation traces and laser spectra of the SWCNT-SAM (Fig. 4(a)) and graphene-SAM (Fig. 4(b)) mode-locked lasers. The central operation wavelength of the mode-locked laser is located around 1050 nm, whereas a spectral bandwidth (FWHM) of 7 and 7.8 nm and pulse duration of 173 and 157 fs are measured for SWCNT-SAM and graphene-SAM, respectively. The measured autocorrelation traces could be well-fitted with a sech²-pulse shape. Taking into account the spectral FWHM bandwidth and pulse duration, the time-bandwidth products for both SAM mode-locked lasers amount to 0.33, indicating nearly Fourier transform-limited pulse performance.

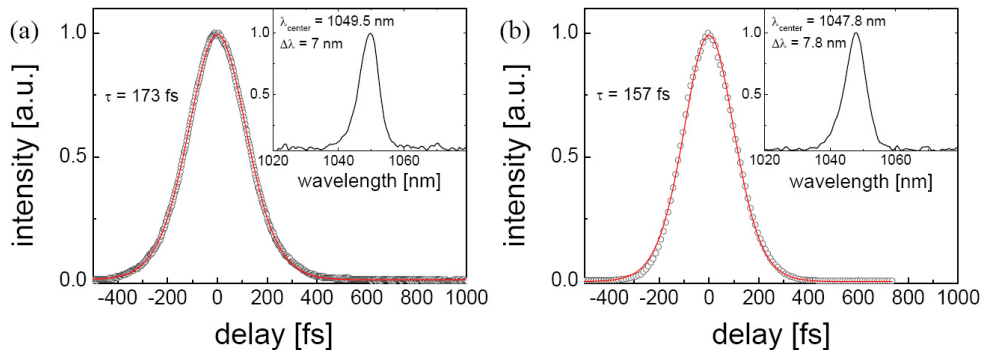


Fig. 4. Autocorrelation traces and laser spectra (insets) of the (a) SWCNT-SAM and (b) graphene-SAM mode-locked Yb:KLuW laser.

Figure 5 shows the radio frequency (RF) spectra of the fundamental beat note at 507.3 and 503.4 MHz recorded with a resolution bandwidth of 1 kHz and the 5-GHz wide-span RF measurements (insets) for the SWCNT-SAM and graphene-SAM mode-locked Yb:KLuW laser. Very high extinction ratios of >80 dBc and the absence of any spurious modulations are evidence for clean single-pulse mode-locking of both SAM mode-locked Yb:KLuW lasers. Lower signal intensities at higher frequencies in the wide-span measurements are attributed to the limited bandwidth of the available photo diode.

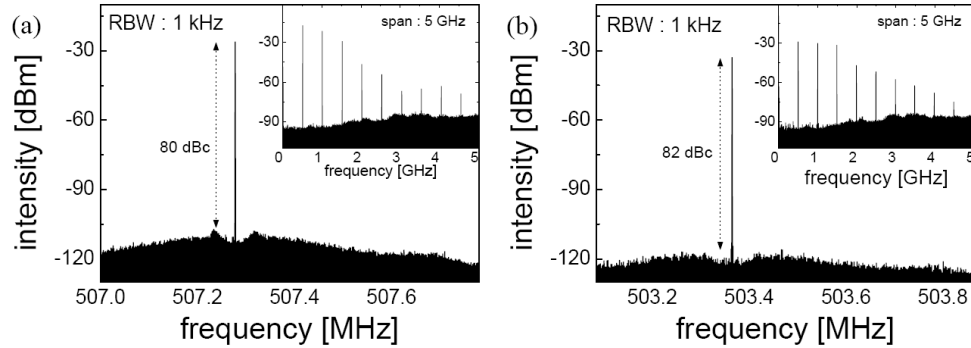


Fig. 5. RF spectra of the fundamental beat note and wide-span measurements (insets) of the (a) SWCNT-SAM and (b) graphene-SAM mode-locked Yb:KLuW laser.

4. Conclusion

We develop a unique carbon nanostructure-based SAM by deposition of SWCNTs and graphene on a single dielectric mirror for the first time and demonstrate its multi-functional application in a diode-pumped 500-MHz mode-locked Yb:KLuW laser operating near 1050 nm. Maximum average output power of up to 85 mW and pulse duration as short as 157 fs are generated with 1% OC. Improvements of the mode-locked laser performance including pulse duration, efficiency, and power scaling are possible by further optimization of SAM parameters and intra-cavity dispersion, output coupling ratio and pump characteristics. Nevertheless, the results achieved in the present work show the potential of diode-pumped carbon nanostructure-mode-locked solid-state lasers as robust and cost-effective solutions for developing >1 GHz repetition rate femtosecond lasers.

Acknowledgments

This work was supported by the National Research Foundation (NRF) of Korea funded by MEST (2011-0017494 and 2008-0061906). This work was also partially supported by the Spanish Government under project MAT2011-29255-C02-02, the Generalitat de Catalunya under project 2009SGR235, and the European Commission within the Seventh Framework Programme under projects Cleanspace and FP7-SPACE-2010-1-GA-263044.